A quantum particle in a circle; an informational approach revisited

E. Cruz[a], N. Aquino[a,*], C. R. Estañón[a] and H. Yee-Madeira[b]

[a]*Departamento de Física, Universidad Autónoma Metropolitana-Iztapalapa,*
Av. Ferrocarril San Rafael Atlixco 186, Iztapalapa, 09310 Ciudad de México, México,
[*]*e-mail: naa@xanum.uam.mx*
[b]*Departamento de Física, Escuela Superior de Física y Matemáticas, Instituto Politécnico Nacional,*
Edificio 9 Ciudad de México, México.
This work is dedicated to the memory of Dr. Víctor David Granados García (1949-2023)

Received 3 September 2024; accepted 14 February 2025

We study the localization-delocalization of a particle moving within an infinite circular well of radius r_0 from a theoretical information point of view. We computed the Shannon entropy, Fisher information and disequilibrium in configuration and momentum spaces for a collection of stationary states. Comparing our results of Shannon entropies with those previously published we found good agreement with those. Shannon entropy, Fisher information and the disequilibrium offer complementary results for the description of the particle localization-delocalization.

Keywords: Particle in a circle; Shannon entropy; Fisher information; disequilibrium.

DOI: https://doi.org/10.31349/RevMexFis.71.040701

1. Introduction

Information theory is an area of constant growth, as shown by the number of papers published each year, and of wide application in various areas of knowledge. Some examples of its applications are: the study of earthquakes [1], image retrieval and indexing [2], cryptography [3], noise theory [4], robot navigation [5], machine learning [6], study of early stone tools [7], black holes [8], etc.

In particular in quantum mechanics it has been used to study free systems and some systems subject to spatial confinement. The Shannon entropy has been used as a measure of electron localization-delocalization in aromatic compounds [9], in atomic and molecular calculations [10-24] and recently, in spatially confined systems such as: the hydrogen atom, helium and multi-electron atoms enclosed within penetrable and impenetrable walled boxes, models that simulate the behaviour of matter under the action of high external pressures.

The particle inside an infinite circular well (ICW) is a simple quantum mechanical example [25-27], but the study of this system is not only of academic interest. Dong *et al.* [28] studied the Shannon entropy in configuration and momentum spaces of a particle in an ICW like a mathematical example. On the other hand, Corzo *et al.* [29] studied the particle inside an ICW as a model of an electron in a circular quantum corral. They calculated the radial Shannon entropy in the configuration and momentum spaces and also they introduced a one dimensional entropy with a more simple structure as a function of the radial and angular quantum numbers. Cruz *et al.* [30] studied an electron inside an ICW in the presence of a magnetic field. Tai *et al.* [31] found by molecular calculations that the cluster B_{20}^{2-} has the shape of a ICW.

Corzo *et al.* [29] and Dong *et al.* [28] analysed the radial standard deviation and radial Shannon entropy of the problem of a quantum particle in an ICW. Corzo *et al.* [29] pointed out that the standard deviation is sensitive to the shape and width of the probability density distribution. This fact is reflected in a study made by Bialynicki-Birula and Rudnicki [32] in which they show that in some very simple physical systems the standard deviation has serious fails in the description of the dispersion of the probability density.

Corzo *et al.* [29] found that the radial standard deviation and the radial Shannon entropy have different behavior. The radial standard deviation of different states as a function of the radial quantum number shows an increase, *i.e.*, it shows a growing in the dispersion in the probability density distribution (delocalization). While the radial Shannon entropy shows a trend towards localization for states with angular momentum $m \leq 4$. They found that the radial Shannon entropy results give a measure consistent with the probability distribution of the analyzed states.

The aim of this work is to study the localization-delocalization of an electron inside an infinite circular well by means of the following information measures: Shannon entropy, Fisher information and disequilibrium, in configuration and momentum spaces. Our interest in using thes informational measures is to know whether these other measures give results equivalent to those of the Shannon entropies reported previously [28,29] or whether additional information is obtained.

The structure of the work is as follows: In Sec. 2, we show the eigenfunctions and eigen–energies of a particle in a circular box. In Sec. 3 we briefly describe the quantum probability density in configuration and momentum spaces and, the informational measures: Shannon entropy, Fisher information and disequilibrium. In Sec. 4 we show the results and analysis of the computed measures. Finally, in Sec. 5 we give our conclusions.

2. Methodology

2.1. Energy and eigenfunctions

This problem has already been adressed by other authors, so we will only give a brief description of it. Consider a particle of mass m_e moving inside a planar circular region of radius r_0 and with impenetrable walls. The Hamiltonian of the system is given by:

$$H = \frac{p^2}{2m_e} + V_c(r), \tag{1}$$

where $V_c(r)$ is the confinement potential of impenetrable wall

$$V_c(r) = \begin{cases} 0 & \text{if} \quad 0 \le r \le r_0 \\ \infty & \text{if} \quad r > r_0 \end{cases}. \tag{2}$$

The Schrödinger equation in polar coordinates (r, ϕ) is the following

$$-\frac{\hbar^2}{2m_e}\left(\frac{1}{r}\frac{\partial}{\partial r}\left(r\frac{\partial}{\partial r}\right) + \frac{1}{r^2}\frac{\partial^2}{\partial \phi^2}\right)\psi(r,\phi) = E\psi(r,\phi). \tag{3}$$

The solutions of this equation are well known [25-31,33],

$$\psi_{n,m}(r,\phi) = R_{n,m}(r)\varphi_m(\phi), \tag{4}$$

where,

$$R_{n,m}(r) = \frac{\sqrt{2}}{r_0 J_{|m|+1}(X_{n,m})} J_m(X_{n,m}\frac{r}{r_0}), \tag{5}$$

and

$$\varphi_m(\phi) = \frac{1}{\sqrt{2\pi}} e^{im\phi}, \tag{6}$$

where n is the radial quantum number $n = 0, 1, 2, 3, \ldots,$ m is the quantum number associated with L_z, $|m| = 0, 1, 2, \ldots$. J_m are the Bessel functions of first kind and order m and $X_{n,|m|}$ is its nth zero [34-36].

The energy eigenvalues are given by:

$$E_{n,m} = \frac{\hbar^2 X^2_{n,|m|}}{2m_e r_0^2}. \tag{7}$$

The states $\psi_{n,m}$ y $\psi_{n,-m}$ are degenerated to the same energy for $m \neq 0$, since $J_{-m} = (-1)^m J_m$ then, J_m and J_{-m} have the same zeros.

In Fig. 1 we show the behaviour of the energy function as a function of the confinement radius r_0.

2.2. The quantum probability density

The probability density in configuration space $\rho(r, \phi)$ is defined as:

$$\rho(r,\phi) = \left|\psi_{n,m}(r,\phi)\right|^2 = \psi^*_{n,m}(r,\phi)\psi_{n,m}(r,\phi), \tag{8}$$

where $\psi(r, \phi)$ is given by Eq. (4). Due to the form of Eq. (4), the probability density is independent of ϕ

$$\rho(r) = \frac{1}{2\pi}\left(\frac{\sqrt{2}}{r_0 J_{|m|+1}(X_{n,m})} J_m(X_{n,m}\frac{r}{r_0})\right)^2, \tag{9}$$

it is also convenient to define the radial probability density $\rho_r(r)$ as follows

$$\rho_r(r) = \int_0^{2\pi} \left|\psi_{n,m}(r,\phi)\right|^2 d\phi. \tag{10}$$

The wave function in momentum space $\Phi_{n,m}(p, \theta)$ is obtained by means of the Fourier transform of the wave function in configuration space, *i.e.*

$$\Phi_{n,m}(p,\theta) = \frac{1}{2\pi}\int_0^{2\pi}\int_0^{r_0} \psi_{n,m}(r,\phi) e^{-i\vec{p}\cdot\vec{r}} r dr d\phi, \tag{11}$$

where $\psi_{n,m}(r, \phi)$ is given by Eq. (4). Then,

$$\Phi_{n,m}(p,\theta) = \frac{1}{(2\pi)^{\frac{3}{2}}} \frac{\sqrt{2}}{r_0 J_{|m|+1}(X_{n,m})} \times \int_0^{2\pi}\int_0^{r_0} J_m(X_{n,m}\frac{r}{r_0}) e^{im\phi} e^{-i\vec{p}\cdot\vec{r}} r dr d\phi, \tag{12}$$

we apply the following identity [34]

$$\int_0^{2\pi} e^{-ikr\cos(\phi - t)} \left\{ \begin{array}{c} \cos(mt) \\ \sin(mt) \end{array} \right\} dt = 2\pi i^m \left\{ \begin{array}{c} \cos(m\phi) \\ \sin(m\phi) \end{array} \right\} J_m(kr). \tag{13}$$

A straightforward calculation gives

$$\Phi_{n,m}(p,\theta) = \frac{i^m e^{im\theta} r_0^2}{\sqrt{2\pi}} \left(\frac{\sqrt{2}}{r_0 J_{|m|+1}(X_{n,|m|})} \times \left\{ \frac{X_{n,|m|} J_{m-1}(X_{n,|m|}) J_m(r_0 p)}{(r_0 p)^2 - X^2_{n,|m|}} \right\} \right). \tag{14}$$

The probability density $\gamma(p, \theta)$ in momentum space is given by

$$\gamma(p,\theta) = \Phi^*_{n,m}(p,\theta)\Phi_{n,m}(p,\theta). \tag{15}$$

3. Entropic measures

The Shannon entropy, Fisher information and disequilibrium, in the position and momentum spaces, describe how concentrated or dispersed the probability density is. The study of these quantities has been used in the analysis of different quantum systems, such as particles, free and confined atoms [10-24,30,37-48].

3.1. Shannon entropy

3.1.1. Configuration space

The Shannon entropy in configuration space is interpreted as the uncertainty in estimating the position of the particle in space.

The definition of the Shannon entropy in the configuration space for the two-dimensional system under analysis is given by:

$$S_\rho = -\int_0^{2\pi}\int_0^{r_0} \rho(r,\phi)\ln\left[\rho(r,\phi)\right] r dr d\phi, \tag{16}$$

where $\rho(r,\phi)$ is given by Eq. (9), so Eq. (16) can be written as,

$$S_\rho = -2\pi\int_0^{r_0} \rho(r)\ln\left[\rho(r)\right] r dr. \tag{17}$$

The Shannon entropy S_ρ is a global measure of the dispersion of the probability density $\rho(\vec{r})$.

3.1.2. Momentum space

The Shannon entropy in momentum space is given by,

$$S_\gamma = -\int_0^{2\pi}\int_0^{\infty} \gamma(p,\theta)\ln\left[\gamma(p,\theta)\right] p dp d\theta, \tag{18}$$

where the probability density in momentum space $\gamma(p,\theta)$ is given by Eq. (15).

Bialynicki-Birula and J. Mycielski (BBM) [49] showed that there is an uncertainty relation between the entropies, S_ρ and S_γ, which for the two-dimensional space is given by

$$S_\rho + S_\gamma \geq 2(1+\ln[\pi]) \geq 4.28946. \tag{19}$$

3.2. Fisher information

3.2.1. Configuration space

For the present system the Fisher information in the configuration space is defined as

$$F_\rho = \int_0^{2\pi}\int_0^{r_0} \frac{|\vec{\nabla}\rho(r,\phi)|^2}{\rho(r,\phi)} r dr d\phi, \tag{20}$$

the probability density $\rho(r,\phi)$ is given by Eq. (8), then, the Fisher information is simplified to

$$F_\rho = 4\int_0^{r_0}\left(\frac{d}{dr}R_{n,m}(r)\right)^2 r dr. \tag{21}$$

The Fisher information F_ρ is a measure of the narrowness of the probability density and it is a local measure of the oscillations of $\rho(\vec{r})$.

3.2.2. Momentum space

The Fisher information in momentum space is given by

$$F_\gamma = \int_0^{2\pi}\int_0^{\infty} \frac{|\vec{\nabla}\gamma(p,\theta)|^2}{\gamma(p,\theta)} p dp d\theta, \tag{22}$$

the probability density $\gamma(p,\theta)$ is given by equation (15), and the wave function $\Phi_{n,m}(p,\theta)$ by equation (14), then

$$F_\gamma = 4r_0^4\int_0^{\infty}\left(\frac{d}{dp}\left(\frac{\sqrt{2}}{r_0 J_{|m|+1}(X_{n,|m|})}\right.\right. \\ \left.\left.\times\left\{\frac{X_{n,|m|}J_{m-1}(X_{n,|m|})J_m(r_0 p)}{(r_0 p)^2 - X_{n,|m|}^2}\right\}\right)\right)^2 p dp. \tag{23}$$

When the wave function in configuration space $\psi(\vec{r})$ is a real function, the Fisher information in position F_ρ and momentum F_γ spaces satisfy the following position–momentum uncertainty relation [50],

$$F_\rho F_\gamma \geq 4N^2, \tag{24}$$

where $N=2$, is the system dimension.

3.2.3. Disequilibrium

The disequilibrium D is also called Onicescu energy or self–similarity [51,52]. The disequilibrium in configuration space D_ρ is defined as:

$$D_\rho = \int \rho^2(\vec{r})d\vec{r}, \tag{25}$$

the disequilibrium gives a measure the separation between two distributions, one of them is the equilibrium density.

The disequilibrium in momentum space is defined as:

$$D_\gamma = \int \gamma^2(\vec{p})d\vec{p}. \tag{26}$$

For a normal probability density the value of the disequilibrium is equal to the inverse of the square root of the variance [53]. If the probability density is very compact the variance is small and the disequilibrium will have a large value and vice versa.

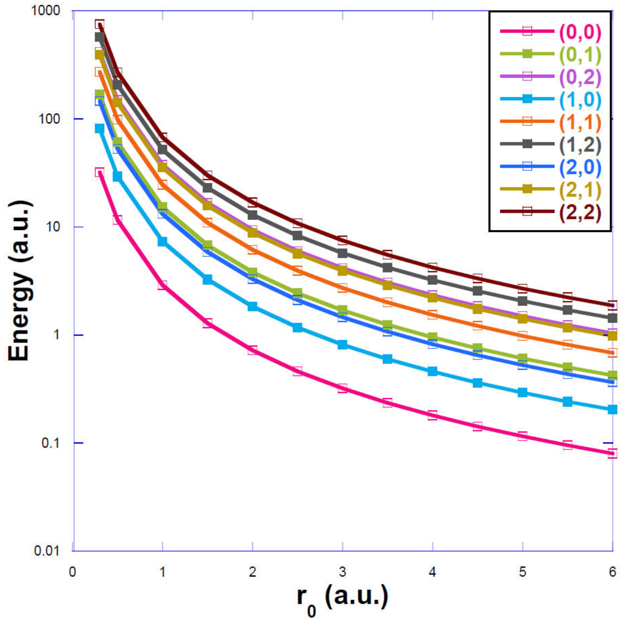

FIGURE 1. Energy eigenvalues for few states (n, m) as a function of the confinement radius r_0. Energy eigenvalues for few states(n, m) as a function of the confinement radius $r_{_0}$.

4. Results

Energy eigenvalues

In Fig. 1 we show the behaviour of energy eigenvalues of few states (n, m) as a function of the confinement radius $r_{_0}$. The energy eigenvalues decrease for all states as the confining radius increases. As the confinement radius grows the uncertainty in the particle position also increases, because the particle has a larger space to move, and by the Heisenberg uncertainty principle, the uncertainty in the linear momentum of the particle decreases. Since the particle has only kinetic energy, it decreases with increasing confinement radius.

For states with $m \neq 0$, they have double degeneracy, *i.e.*, $E_{_{n,-m}} = E_{_{n,m}}$.

Shannon entropy

The Shannon entropy, in either of the two spaces, cannot be obtained in analytical form, to obtain its values we used numerical integration by means of the Mathematica 13 program. For Shannon entropy, Fisher information and disequilibrium, in the momentum space we replace the upper limit of integration '∞' in Eqs. (18) and (23) by $p_{\max}$. To obtain the value of $p_{\max}$ we use the normalization criterion, since we know that the wave function in the momentum space $\Phi_{_{n,m}}(p, \theta)$ is normalized to unity. Therefore, we choose the value of $p_{\max}$ at which the result of the normalization integral is:

$$\int_0^{2\pi} \int_0^{p_{\max}} \Phi^*_{_{n,m}}(p, \theta)\Phi_{_{n,m}}(p, \theta) p dp d\theta = 0.999999, \quad (27)$$

we found that $p_{\max} = 300$ is enough in all the studied states.

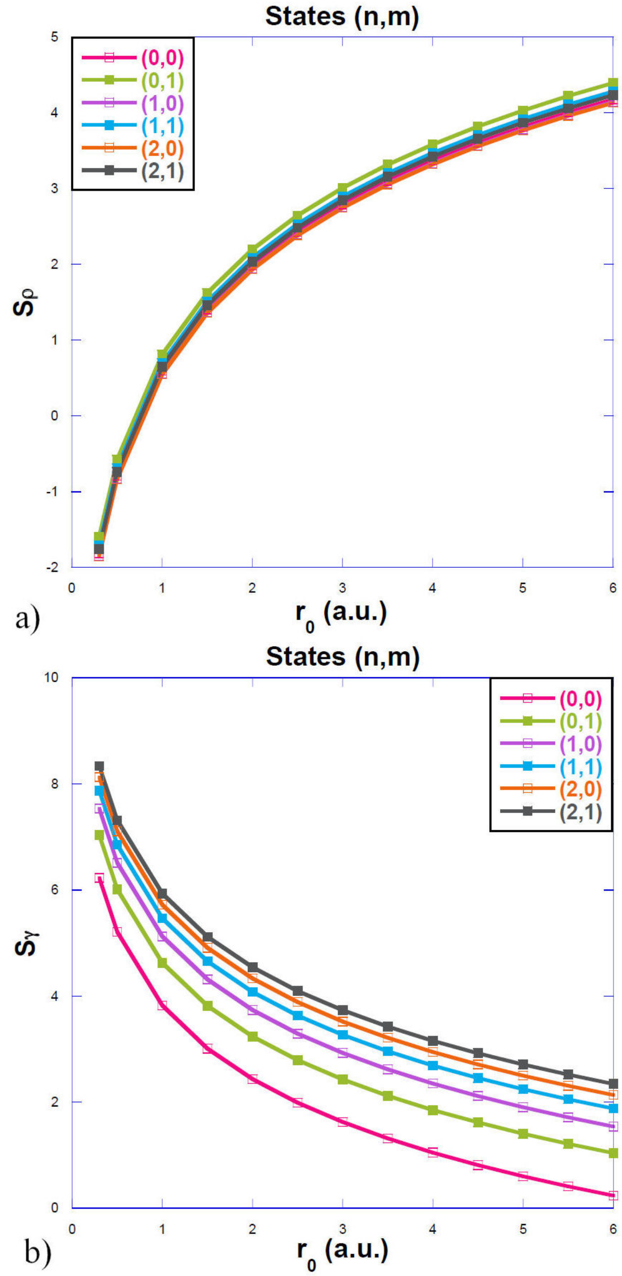

FIGURE 2. Shannon entropy in configuration S_ρ and momentum S_γ space as a function of the confinement radius $r_{_0}$.

In Fig. 2 we show the behaviour of the Shannon entropy as a function of the confinement radius r_0. In Fig. 2a) is shown that the Shannon entropy in the configuration space increases (delocalization) when r_0 grows. In Fig. 2b) is shown that the Shannon entropy in momentum space decreases (localization) as r_0 grows, this indicates that the probability density in the momentum space is more compact. Whereas when r_0 diminishes the Shannon entropy in the configuration space decreases (localization) and in the momentum space it increases (delocalization). The behavior of the Shannon entropy S_ρ in configuration space shown in Fig. 2a) is in full agreement with the results of Ref. [28]. However, the behav-

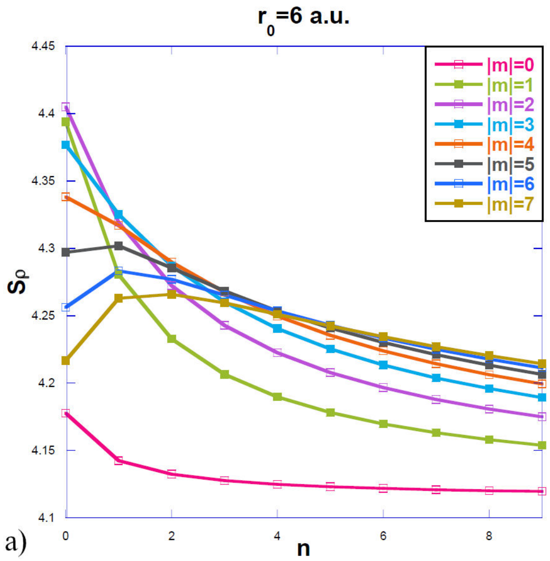

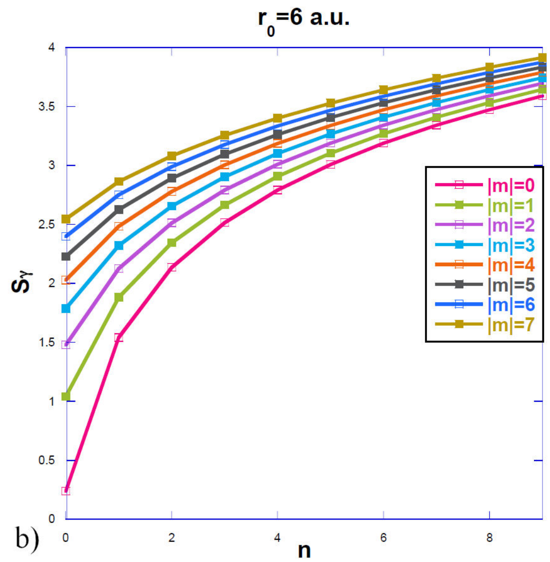

FIGURE 3. Variation of Shannon entropy in position and momentum space varying the quantum numbers n and m, for a confinement radius of 6 a.u.

ior of the Shannon entropy in the momentum space S_γ shown in Fig. 2b) and the results of Ref. [28] are somewhat different, the results obtained in Ref. [28] show strong variations as a function of r_0, while in the Fig. 2a) the curves of S_γ are smooth.

Figure 3 shows the behavior of the Shannon entropy as a function of the radial quantum number n for different values of the angular momentum m, for a fixed confining radius $r_0 = 6$ a.u. The Shannon entropy in configuration space S_ρ for the states with $|m| = 0, 1, 2, 3$ and 4 decreases faster as n increases, indicating more localization with the increment of the radial nodes. On the other hand, for states with angular momentum $|m| = 5, 6$ and 7 the behavior of S_ρ indicates first a delocalization of the particle, then, by continuing to increase the quantum number n, the particle tends to be more localized in this space. The Shannon entropy in momentum space S_γ shows a delocalization of the particle as the number of radial nodes increases. The behaviour of Shannon entropy in configuration space S_ρ of Fig. 3 is the same found by Corzo *et al*. [29]. Unfortunately, they do not calculate the radial Shannon entropy in momentum space. Figure 4 shows the radial density $\rho_r(r)$ for a collection of states (n, m) for a fixed value $r_0 = 6$ a.u., this figure is analogous to Fig. 3 of Ref. [29]. The Fig. 4 is useful to interpret the results of the Shannon entropy of this system. The rows of Fig. 4 have a fixed quantum number m, in the first column $n = 0$, in the next column $n = 1$ and in the third column $n = 2$. In the first column of Fig. 4, $n = 0$, as the value of m increases the radial probability density becomes more compact (localization), which is consistent with the Shannon entropy for the curve with $n = 0$ as a function of m, (Fig. 5).

Figure 5 shows the behavior of the Shannon entropy as a function of the angular momentum quantum number m, for ten values of the radial quantum number n, maintaining a fixed radius $r_0 = 6$ a.u.. The Shannon entropy in the configuration space S_ρ, for states with $n = 0$, 1 and 2, increases fast, indicating a delocalization of the particle, as m continues to increase the Shannon entropy decreases, indicating further spatial localization. The Shannon entropy for states with $n > 2$ increases slowly, and as shown by Corzo *et al*. [29], this entropy tends to decrease for values of m greater than 10. On the other hand, the Shannon entropy in the momentum space S_γ increases slowly with increasing m indicating a delocalization in the momentum space.

In Fig. 6 we show the Shannon entropy in configuration and momentum spaces and the entropic sum $S_t = S_\rho + S_\gamma$ as a function of the confinement radius r_0. The Shannon entropies S_ρ and S_γ are symmetric with respect to each other, when one increases the other decreases in the same proportion, this results in the total entropy remaining constant as a function of r_0. The total entropy satisfies the BBM uncertainty relation (19).

Fisher information

In Fig. 7 left, we show the behaviour of the Fisher information F_ρ in configuration space, and in Fig. 7 right the Fisher information F_γ in momentum space, as a function of the confining radius r_0. It is observed that for these states the Fisher information in the configuration space decreases as the confinement radius increases, indicating a delocalization of the probability density and as a consequence the uncertainty increases when estimating the particle position. In contrast, the Fisher information in the momentum space increases with increasing confinement radius, indicating that the probability density in this space is more concentrated.

Figure 8 shows the behavior of Fisher information in configuration and momentum spaces as a function of radial quantum number n for eight different values of the angular momentum m, for a fixed radius $r_0 = 6$ a.u. The Fisher in-

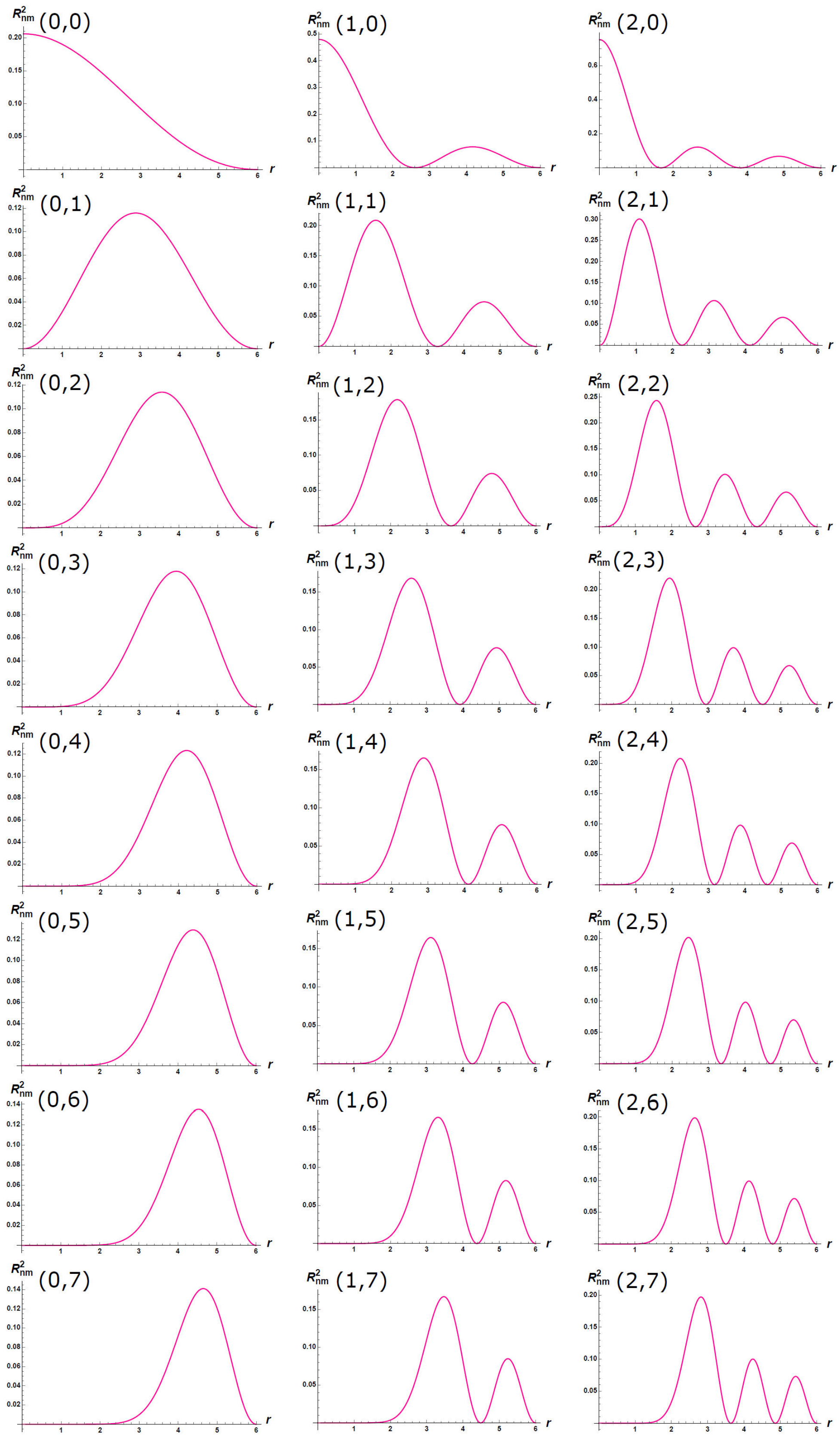

FIGURE 4. Radial density R^2_{nm} for the states (n, m) for a fixed confinement radius $r_0 = 6$ a.u.

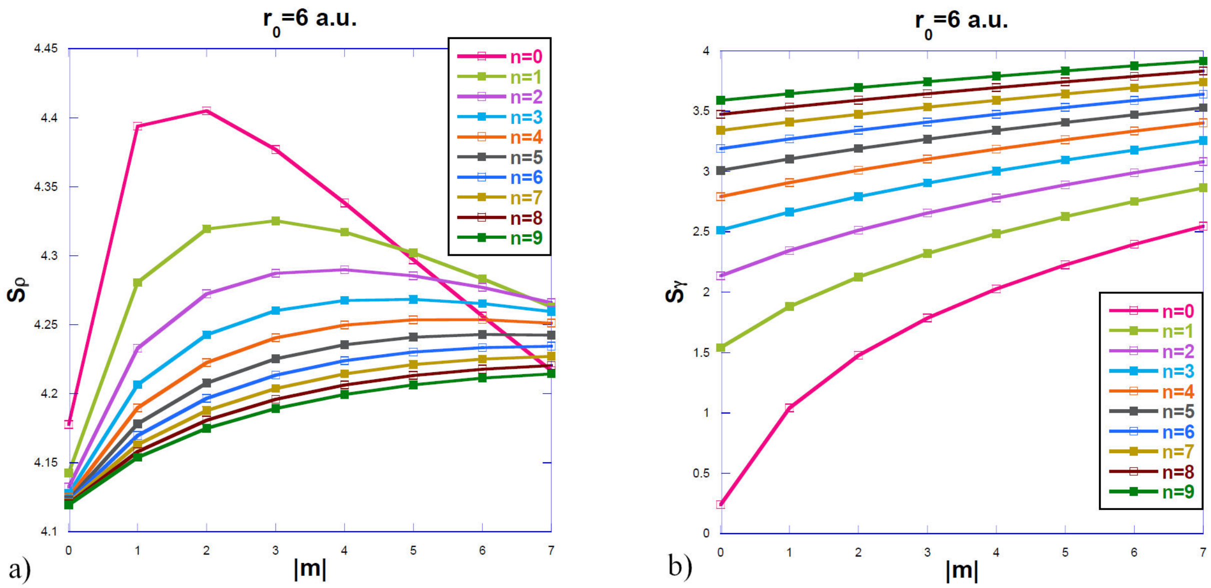

FIGURE 5. Variation of Shannon entropy in position and momentum space varying the quantum numbers m and n, for a confinement radius of 6 a.u.

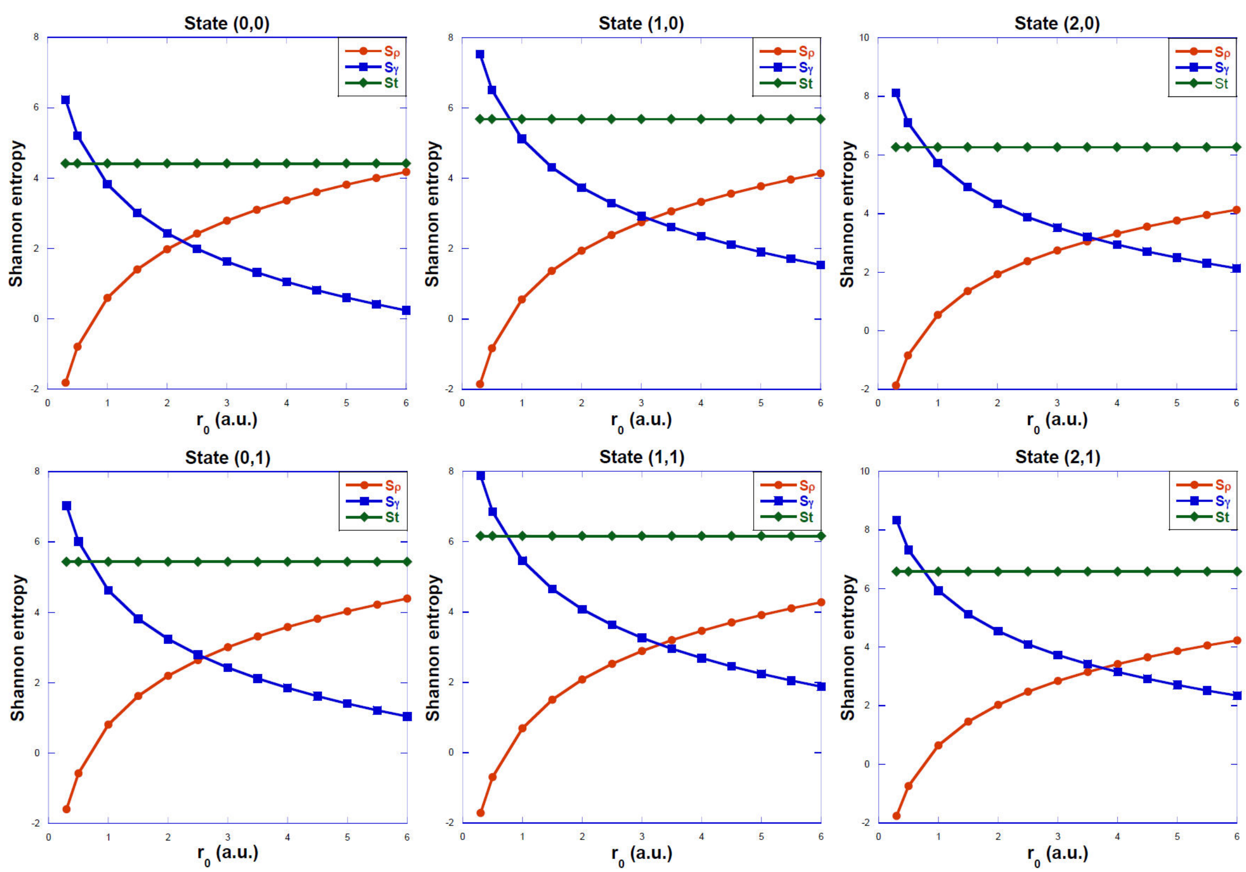

FIGURE 6. The Shannon entropy in configuration and momentum spaces, and the total entropy for different states (n, m) as a function of the confinement radius r_0.

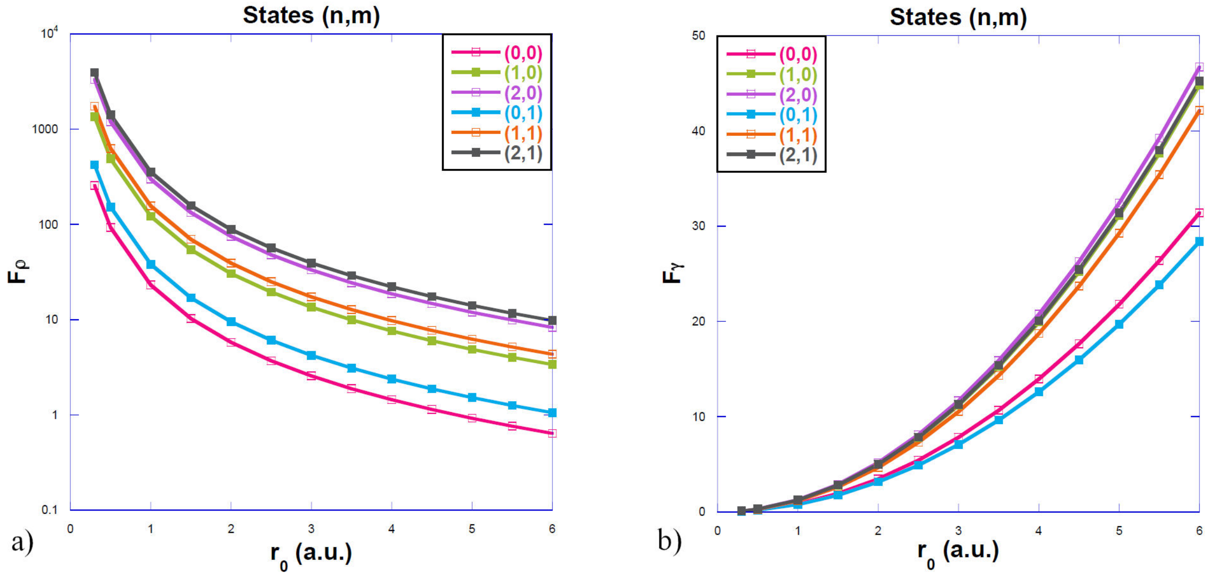

FIGURE 7. Fisher information in configuration and momentum spaces for different states (n, m) as a function of the confining radius r_0.

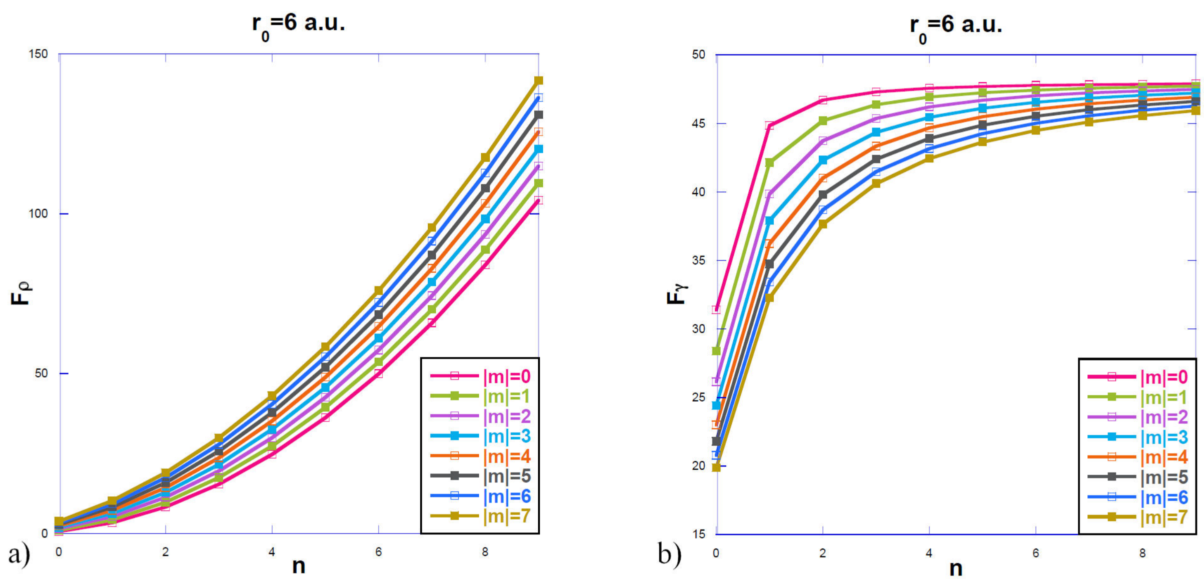

FIGURE 8. Variation of Fisher information in position and momentum space varying the quantum numbers n and m, for a confinement radius of 6 a.u.

formation in configuration space F_ρ grows as n increases. The Fisher information in momentum space F_γ also increases with n but quickly reaches its asymptotic limit.

Figure 9 shows the Fisher information in configuration and momentum spaces as a function of the angular momentum m for different values of the radial quantum number n, for a fixed value of r_0. In configuration space F_ρ grows as a function of m, whereas, in the momentum space F_γ diminishes, as expected.

In Fig. 10 we show the Fisher information in configuration and momentum spaces for six different states (n, m), as a function of the confinement radius r_0. Note the very symmetrical behavior between F_ρ and $F\gamma$. The Fisher information in configuration space F_ρ decreases, whereas, in the momentum space $F\gamma$ increases as r_0 grows. The product $F_\rho F\gamma$ remains constant as the confinement radius r_0 increases. We must remember that wave functions [Eq. (4)] with $m \neq 0$ are not real-valued functions, however, the relation (24) is satisfied.

Disequilibrium

As we mentioned in Sect. 3.2.3, for a normal probability density the value of the disequilibrium is equal to the inverse of the variance. When the probability density is very compact the variance is small and the disequilibrium will have a large value and vice versa. The probability densities studied in this paper are not normal densities but still in this case the disequilibrium gives a measure of how dispersed these probability densities are. A large value of the disequilibrium is

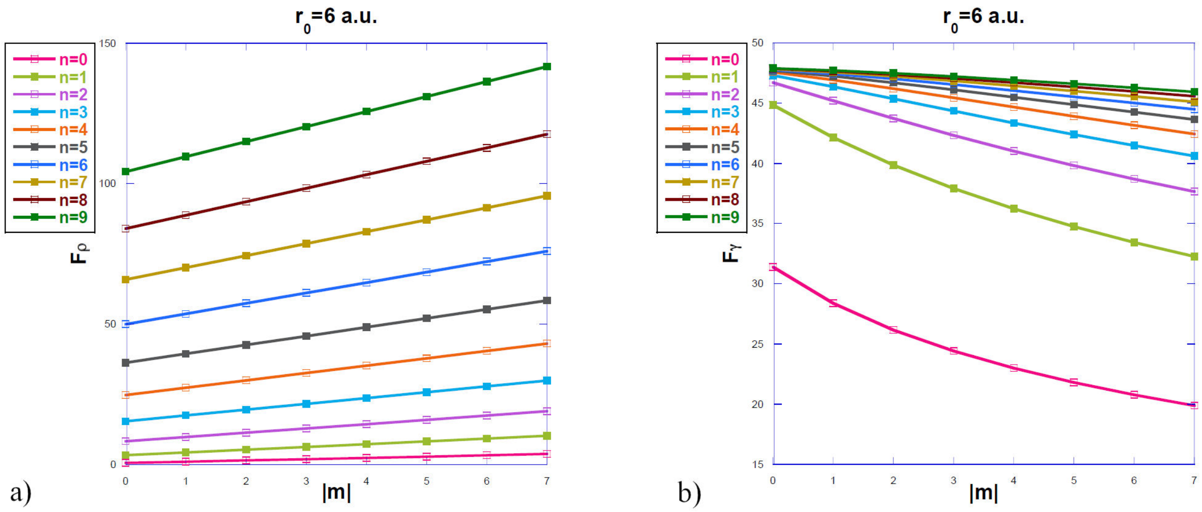

FIGURE 9. Variation of Fisher information in position and momentum space varying the quantum numbers m and n, for a confinement radius of 6 a.u.

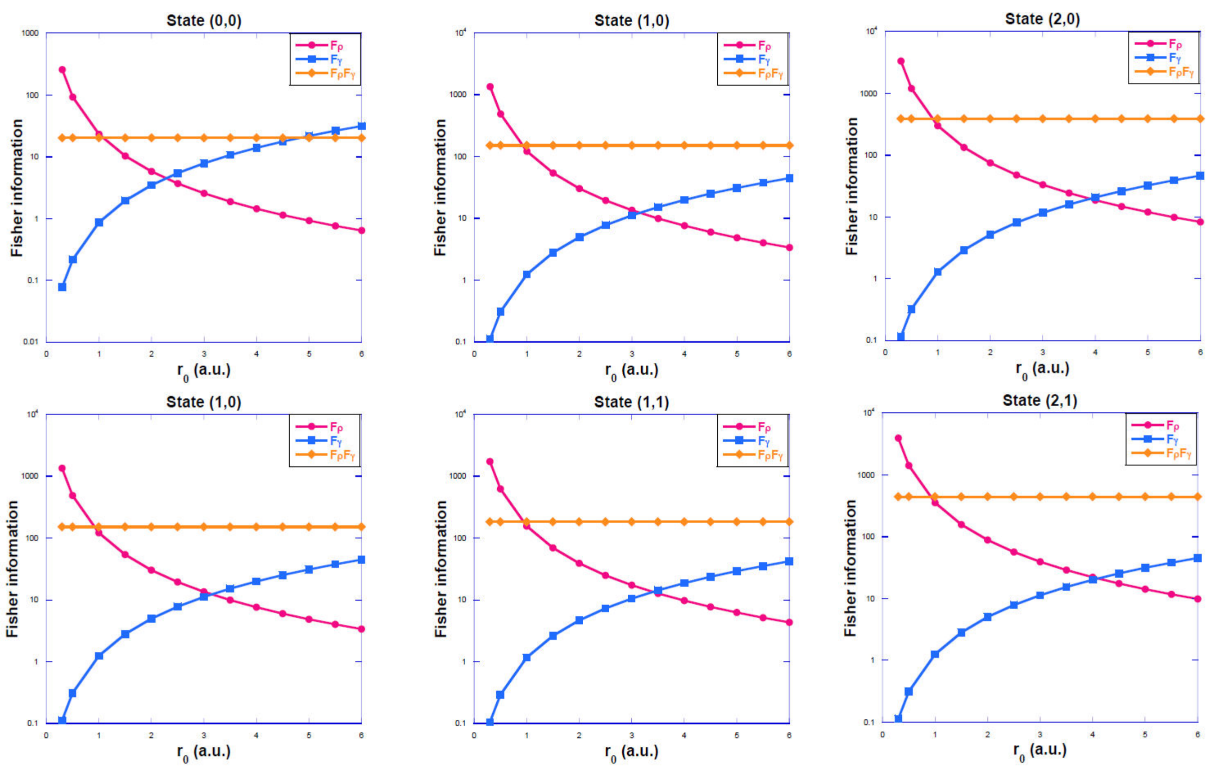

FIGURE 10. Fisher information in the configuration F_ρ and momentum spaces F_γ, and the information product $F_\rho F_\gamma$ for states (n, m) as a function of the confinement radius r_0.

interpreted as localization, while a small value will be delocalization. In Fig. 11 we show the disequilibrium in configuration and momentum spaces. As the confining radius diminishes the value of the disequilibrium in configuration space D_ρ increases, this means that the probability density of all states (n, m) becomes more compact (localization). On the other hand, in the momentum space the desiquilibrium D_γ decreases (delocalization) as r_0 diminishes. When r_0 grows the values of D_ρ decrease (delocalization) and the values of D_γ increase (localization). Figures 11 and 7 of the Fisher information show certain similarity. The results obtained with the disequilibrium are in complete agreement with those obtained with the Shannon entropy and Fisher information.

In Fig. 12 is shown the disequilibrium as a function of radial quantum number n in the configuration and momentum

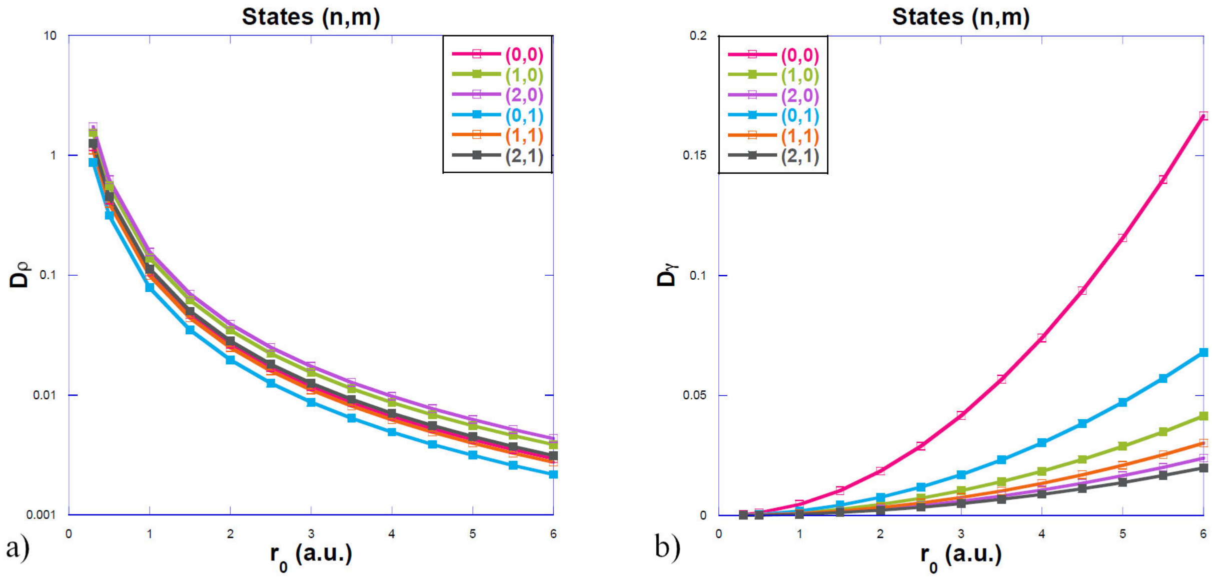

FIGURE 11. Disequilibrium in configuration and momentum spaces for different states (n, m) as a function of the confining radius r_0.

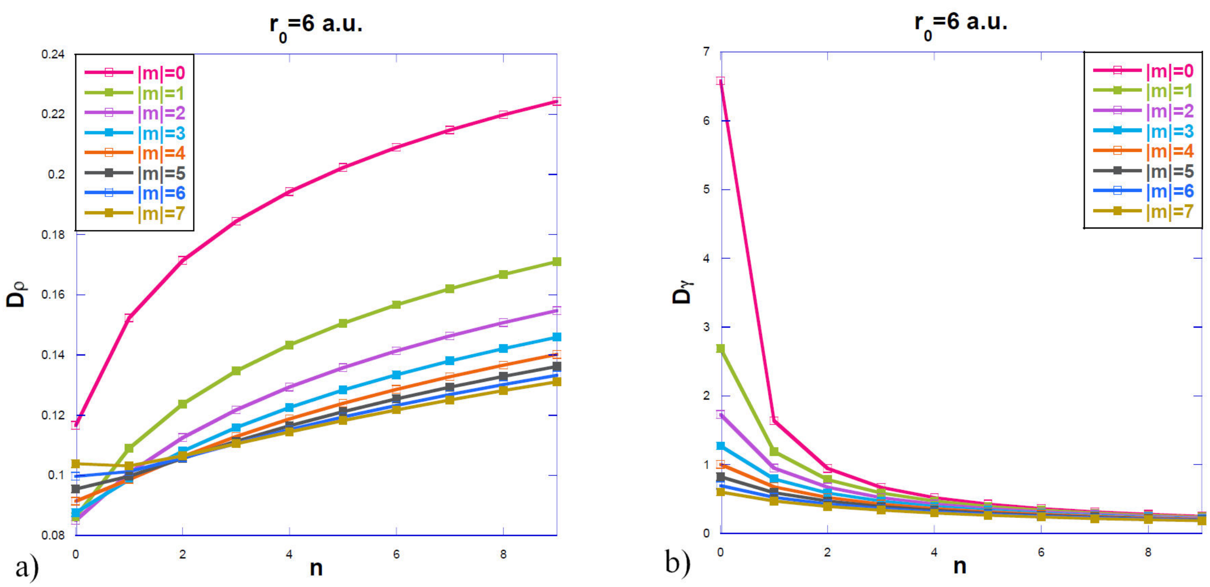

FIGURE 12. Disequilibrium in configuration and momentum spaces as a function of the quantum numbers n for different quantum numbers m for a confinement radius of 6 a.u.

spaces, each curve representing states with the same angular momentum quantum number m. The disequilibrium in configuration space $D\rho$, of state (n, m) will be denoted as $D\rho(n, m)$. We see from Fig. 12 , $D\rho(0, 0) > D\rho(0, 7) > D\rho(0, 6)$, etc. This order changes as n increases, as for example, for $n > 2$, the order is $D\rho(n, 7) < D\rho(n, 6) < D\rho(n, 5) \cdots < D\rho(n, 0)$ and the values of D_ρ increases (localization) for all states. On the other hand, the disequilibrium in momentum space is always a decreasing function of n (delocalization).

In Fig. 13 is shown the disequilibrium as a function of angular quantum number m in the configuration and momentum spaces, each curve representing states with the same radial quantum number n. The disequilibrium in the configuration space, for states with $n = 0$, 1 and 2, first decreases (delocalization) reaches a minimum value and then slowly increases (localization) as a function of m. For states with $n > 2$, the disequilibrium decreases (delocalization) as $|m|$ grows from 0 to 7. The disequilibrium in the momentum space decreases (delocalization) as m increases.

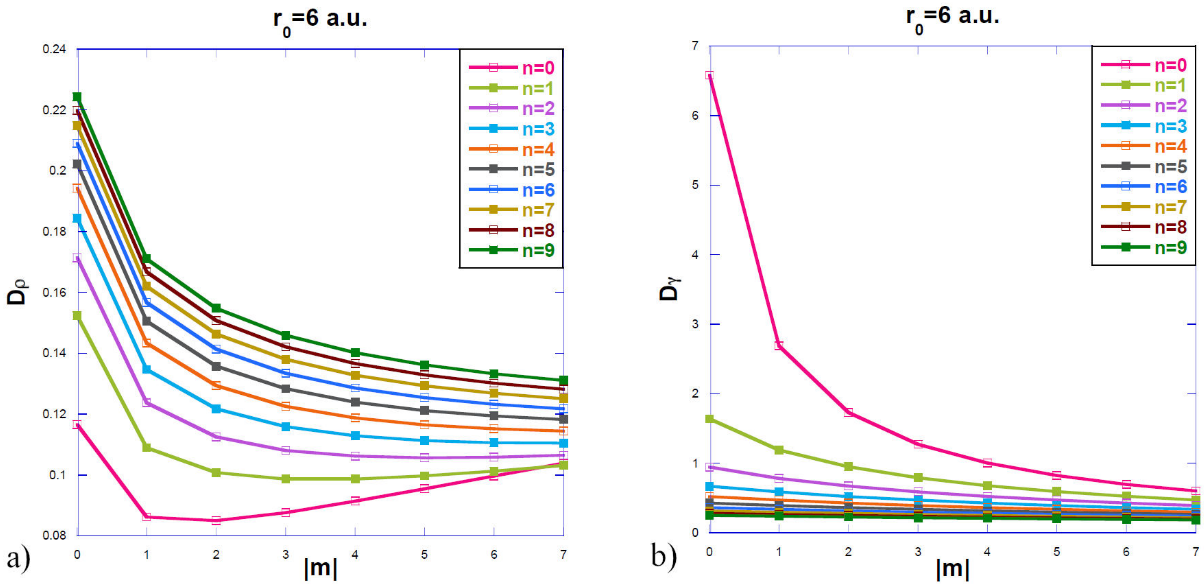

FIGURE 13. Disequilibrium in configuration and momentum spaces as a function of the quantum numbers m for different quantum numbers n for a confinement radius of 6 a.u.

5. Conclusions

We studied a particle confined in a circular region of radius r_0, we show that the eigenenergies of the states (n, m) show a decreasing behaviour with increasing of r_0, as it would be expected physically (as a consequence of the Heisenberg Uncertainty Principle, as we mentioned above).

We used the Shannon entropy, Fisher information and disequilibrium as measures of localization-delocalization of the confined particle in a circular region.

In the configuration space the particle delocalizes as the confining radius increases, while in the momentum space the particle tends to localize. These results were to be expected physically, since as the confining radius increases the region in which the quantum particle is located becomes larger, increasing the uncertainty in the position of the particle and reducing the uncertainty in its momentum, in agreement with the Heisenberg uncertainty principle.

For fixed values of the confining radius r_0 and the angular momentum quantum number m the following was found: 1) The Shannon entropy in the configuration space as a function of the radial quantum number n decreases (localization), whereas in the momentum space the opposite occurs, the Shannon entropy increases (delocalization). 2) The Fisher information in the configuration space and in the momentum space increase as a function of the radial quantum number n. 3) The disequilibrium in the configuration space grows (localization), while in the momentum space it decreases (delocalization), as the radial quantum number n increases.

For a fixed value of the confining radius r_0 and the radial quantum number n we found the following: 1) For states with $n = 0$, 1 and 2 the Shannon entropy in configuration space, first increases (delocalization), reaches a maximum and then decreases (localization) as $|m|$ grows. Whereas for the other states this entropy always increases slowly (delocalization). The Shannon entropy in momentum space is always an increasing function (delocalization) of $|m|$. 2) The Fisher information in configuration space is an increasing function of $|m|$ for $n = 0$, 1,...,9. Whereas Fisher information in momentum spaces is always a decreasing function of $|m|$. On the other hand, the disequilibrium in configuration space as a function of $|m|$, for the states with $n = 0$, 1 and 2, first decrease (delocalization), reaches a minimum and then increase (localization) slowly. For the other states D_ρ always decreases (delocalization). The disequilibrium in momentum space decreases (delocalization) as $|m|$ increases.

In this work we have reproduced the behavior of the Shannon entropy obtained previously [28,29], and we have extended the study using the Fisher information and disequilibrium in configuration and momentum spaces.

1. Y. Wang, Seismic Inversion: Theory and Applications. (Wiley Blackwell: Hoboken, NJ, USA, 2016).

2. A. Srivastava, Stochastic models for capturing image variability. *IEEE Signal Process. Mag.*, **19** (2002) 63, `https://doi.org/10.1109/MSP.2002.1028353`.

3. F. Grosshans and N. J. Cerf, Continuous-variable quantum cryptography is secure against non-gaussian attacks. *Phys. Rev. Lett.*, **92** (2004) 047905, `https://doi.org/10.1103/PhysRevLett.92.047905`.

4. A. D. Wyner and S. Shamai, Introduction to communica-

tion in the presence of noise by c. e. shannon. *Proc. IEEE*, **86** (1998) 442, https://doi.org/10.1109/jproc.1998.659496.

5. J. Huang, T. Supaongprapa, I. Terakura, F. Wang, N. Ohnishi, and N. Sugie, A model-based sound localization system and its application to robot navigation. *Rob. Aut. Syst.*, **27** (1999) 199, https://doi.org/10.1016/S0921-8890(99)00002-0.
6. M. Prato and L. Zanni, Inverse problems in machine learning: An application to brain activity interpretation. *J. Phys.: Conf. Ser.*, **135** (2008) 012085, https://doi.org/10.1088/1742-6596/135/1/012085.
7. F. del Rio, R. López-Hernández, and C. Chaparro-Velázquez, On information, entropy, and early stone tools. *Mol. Phys.*, **e2310644** (2024) 00268976, https://doi.org/10.1080/00268976.2024.2310644.
8. R. Casadio, R. da Rocha, P. Meert, L. Tabarroni, and W. Barreto, Configurational entropy of black holes quantum cores. *Class. Quantum Grav.*, **40** (2023) 075014, https://doi.org/10.1088/1361-6382/acbe89.
9. Z. Chen, C. S.Wannere Corminboeuf, R. Puchta, and P. R. V. Schleyer, Nucleus-independent chemical shifts (ncis) as an aromaticity criterion. *Chem. Rev.*, **105** (2005) 3842, https://doi.org/10.1021/cr030088+.
10. G. Maroulis, M. Sana, and G. Leroy, Molecular properties and basis set quality: An approach based on information theory. *Int. J. Quantum Chem.*, **19** (1981) 43, https://doi.org/10.1002/qua.560190106.
11. A. M. Simas, A. J. Takkar, and V. H. Smith, Basis set quality, ii. information theoretic apparaisal of various s-orbitals. *Int. J. Quantum Chem.*, **24** (1983) 527, https://doi.org/10.1002/qua.560240603.
12. S. R. Gadre, S. B. Sears, S. J. Chakravorty, and R. B. Bendale, Some novel characteristics of atomic information entropies. *Phys. Rev. A*, **32** (1985) 2602, https://doi.org/10.1103/PhysRevA.32.2602.
13. M. Ho, R. P. Sagar, H. Schmider, D. F. Weaver, and B. H. Smith Jr., Measures of distance for atomic charge and momentum densities and their relationship to physical properties. *Int. J. Quantum Chem.*, **53** (1994) 627, https://doi.org/10.1002/qua.560530606.
14. P. Fuentealba and J. Melin, Atomic spin density polarization index and atomic spin-density information entropy distance. *Int. J. Quantum Chem.*, **90** (2002) 334, https://doi.org/10.1002/qua.994.
15. R. Atre, A. Kumar, and R. P. Panigraph, Quantum information entropies of the eigenstates and the coherent state of the pöschl-teller potential. *Phys. Rev. A*, **69** (2004) 052107, https://doi.org/10.1103/PhysRevA.69.052107.
16. J. S. Dehesa, A. Martinez-Finkelstein, and V. N. Sorokin. Information theoretic measures for morse and pöschl-teller potentials. *Mol. Phys.*, **104** (2006) 613, https://doi.org/10.1080/00268970500493243.
17. M. W. Coffey, Semiclassical position and momentum information entropy for sech2 and a family of rotational potentials. *Can. J. Phys.*, **85** (2013) 733, https://doi.org/10.1139/p07-062.
18. G. H. Sun and S. H. Dong, Quantum information entropies of the eigenstates for a symmetrically trigonometric rosen-morse potential. *Phys. Scr.*, **87** (2013) 045003, https://doi.org/10.1088/0031-8949/87/04/045003.
19. G. H. Sun, S. H. Dong, and S. Naad, Quantum information entropies for an asymmetric trigonometric rosen-morse potential. *Ann. Phys.* (Berlin), **525** (2013) 934, https://doi.org/10.1002/andp.201300089.
20. E. Aydiner, C. Orta, and R. Sever, Quantum information entropies of the eigenstates of the morse potential, *Int. J. Mod. Phys. B*, **22** (2008) 231, https://doi.org/10.1142/S021797920803848X.
21. I. Nasser and A. Abdel-Hady, Fisher information and Shannon entropy calculations for two-electron systems. *Can. J. Phys.*, **98** (2020) 784, https://doi.org/10.1139/cjp-2019-0391.
22. I. Nasser, C. Martínez-Flores, M. Zeama, R. Vargas, and J. Garza. Tsallis entropy: A comparative study for the 1s2-state of helium atom. *Phys. Lett. A*, **392** (2021) 127136, https://doi.org/10.1016/j.physleta.2020.127136.
23. R. Joshi, N. Verma, and M. Mohan, Shannon entropy along hydrogen isoelectronic sequence using numerov method. *Rev. Mex. Fís.*, **69** (2023) 060401, https://doi.org/10.31349/RevMexFis.69.060401.
24. R. González-Férez and J. S. Dehesa, Characterization of atomic avoided crossings by means of Fisher's information. *The European Physical Journal D*, **32** (2005) 39, https://doi.org/10.1140/epjd/e2004-00182-3.
25. R. W. Robinet, Visualizing the solutions for the circular infinite well in quantum and classical mechanics, *Am. J. Phys.*, **64** (1996) 440, https://doi.org/10.1119/1.18188.
26. R. W. Robinet, Visualizing the solutions for the circular infinite well in quantum and classical mechanics. *Am. J. Phys.*, **64** (1996) 440,
27. R. Y. Agcali, B. Atik, E. Bilgen, B. Karli, and M. F. Danisman, Leading to a better understanding of the particle-in-a-quantum-corral model. *J. Chem. Educ.*, **96** (2019) 82, https://doi.org/10.1021/acs.jchemed.8b00622.
28. X. D. Song, G. H. Sun, and S. H. Dong, Shannon information entropy for an infinite circular well. *Physics Letters A*, **379** (2015) 1402, https://doi.org/10.1016/j.physleta.2015.03.020.
29. H. H. Corzo, E. Castaño, H. G. Laguna, and R. P. Sagar, Measuring localization-delocalization phenomena in a quantum corral. *J. Math Chem*, **51** (2012) 179, https://doi.org/10.1007/s10910-012-0073-z.
30. E. Cruz, N. Aquino, and V. Prasad, Localization-delocalization of a particle in a quantum corral in presence of a constant magnetic field. *Eur. Phys. J. D*, **75** (2021) 106, https://doi.org/10.1140/epjd/s10053-021-00119-2.
31. T. B. Tai, R. W. A. Havenith, J. L. Teunissen, A. R. Dok, S. D. Hallaert, M. T. Nguyen, and A. Ceulemans, Particle on a boron disk: Ring currents and disk aromaticity in B_{2-}^{20}, *Inorganic Chemistry*, **52** (2013) 10595, https://doi.org/10.1021/ic401596s.

32. I. Bialynicki-Birula and Rudnicki, Entropic uncertainty relations in quantum physics in K. D. Sen (editor), Statistical Complexity; applica- tions in electronic structure. (Springer, London, 2011), Chap. 1.

33. N. Aquino and E. Casta no, La partícula dentro de una caja circular. *Contactos*, **26** (1998) 11,

34. J. Rey Pastor and A. de Castro Brzezicki, Funciones de Bessel, teoría matemática y aplicaciones a la ciencia y a la técnica. (Ed. DOSSAT S. A., Espa na 1958).

35. M. Abramowitz and I. A. Stegun, Handbook of Mathematical Functions, Chap. 9. (Dover Publications INC, New York, 1972).

36. NIST digital library of Mathematical Functions, Chap. 10. https://dlmf.nist.gov/.

37. W. S. Nascimento and F. V. Prudente, Shannon entropy: A study of confined hydrogenic-like atoms. *Chem. Phys. Lett.*, **691** (2018) 401, `https://doi.org/10.1016/j.cplett.2017.11.048`.

38. Neetik Mukherjee, Sangita Majumdar, and Amlan K. Roy. Fisher information in confined hydrogen-like ions. *Chem. Phys. Lett.*, **691** (2018) 449, `https://doi.org/10.1016/j.cplett.2017.11.059`.

39. K. D. Sen, Characteristic features of shannon information entropy of confined atoms. *J. Chem. Phys.*, **123** (2005) 074110, `https://doi.org/10.1063/1.2008212`.

40. N. Aquino, A. Flores-Riveros, and J. F. Rivas-Silva, Shannon and fisher entropies for a hydrogen atom under soft spherical confinement. *Phys. Lett. A.*, **377** (2013) 2062, `https://doi.org/10.1016/j.physleta.2013.05.048`.

41. M. Rodríguez Bautista, R. Vargas, N. Aquino, and J.Garza, Electrondensity delocalization in many-electron atoms confined by penetrable walls: A hartree-fock study. *Int. J. Quantum Chem.*, **118** (2017) e25571, `https://doi.org/10.1002/qua.25571`.

42. C. R. Estañon, N. Aquino, D. Puertas-Centeno, and J. S. Dehesa, Twodimensional confined hydrogen: An entropy and complexity approach. *Int. J. Quantum Chem.*, **120** (2020) e26192, `https://doi.org/10.1002/qua.26192`.

43. W. S. Nascimento and F. V. Prudente, Sobre um estudo da entropía de shannon no contexto da mecánica quántica: uma aplicacao ao oscilador harmónico livre e confinado. *Quim Nova*, **39** (2016) 757, `https://doi.org/10.5935/0100-4042.20160045`.

44. C. R. Esta non, H. E. Montgomery Jr., J. C. Angulo, and N. Aquino, The confined helium atom: An information-theoretic approach. *Int. J. Quantum Chem.*, **124** (2024) e27358, `https://doi.org/10.1002/qua.27358`.

45. S. Majumdar and A. K. Roy, Shannon entropy in confined helium-like ions within a density functional formalism. *Quantum Rep.*, **2** (2020) 189, `https://doi.org/10.3390/quantum2010012`.

46. I. Nasser, M. Zeama, and A. Abdel-Hady, Renyi, fisher, shannon and their electron correlation tools for two-electron series. *Phys. Scr*. **95** (2020) 095401, `https://doi.org/10.1088/1402-4896/abaa09`.

47. C. Martínez-Flores, Shannon entropy and fisher information for endohedral one an two-electron atoms. *Phys. Lett. A*, **386** (2021) 126988, url-https://doi.org/10.1016/j.physleta.2020.126988.

48. F. C. E. Lima, A. R. P. Moreira, C. A. S. Almeida, C. O. Edet, and N. Ali. Quantum information entropy of a particle trapped by the aharonov-bohmtype effect, *Phys. Scr.*, **98** (2023) 065111, `https://doi.org/10.1088/1402-4896/acd309`.

49. I. Bialynicki-Birula and J. Mycielski, Uncertainty relations for information entropy in wave mechanics. *Commun. Math. Phys.*, **44** (1975) 129, `https://doi.org/10.1007/BF01608825`.

50. P. Sánchez-Moreno, A. R. Plastino, and J. S. Dehesa, A quantum uncertainty relation based on Fisher's information. *J. Phys. A: Math. Theor.*, **44** (2011) 065301, `https://doi.org/10.1088/1751-8113/44/6/065301`.

51. S. López-Rosa, J. C. Angulo, and J. Antolin, Rigorous properties and uncertainty-like relationships on product-complexity measures: Aplication to atomic systems. *Physica A*, **388** (2009) 2081, `https://doi.org/10.1016/j.physa.2009.01.037`.

52. O. Onicescu. C. R. Acad, Theorie de l'information energie informationelle, *Sci. Paris A*, **263** (1966) 25,

53. J. C. Angulo, J. Antolín, and K. D. Sen, Fisher-shannon plane and statistical complexity of atoms. *Physics Letters A*, **372** (2008) 670, `https://doi.org/10.1016/j.physleta.2007.07.077`.